Selective alignment of brain responses by task demands during semantic processing

Giosuè Baggio [a,b,*]

[a] SISSA International School for Advanced Studies, via Bonomea 265, 34136 Trieste, Italy
[b] Max Planck Institute for Psycholinguistics, Wundtlaan 1, 6525 XD Nijmegen, The Netherlands

ABSTRACT

The way the brain binds together words to form sentences may depend on whether and how the arising cognitive representation is to be used in behavior. The amplitude of the N400 effect in event-related brain potentials is inversely correlated with the degree of fit of a word's meaning into a semantic representation of the preceding discourse. This study reports a double dissociation in the latency characteristics of the N400 effect depending on task demands. When participants silently read words in a sentence context, without issuing a relevant overt response, greater temporal alignment over recording sites occurs for N400 onsets than peaks. If however a behavior is produced – here pressing a button in a binary probe selection task – exactly the opposite pattern is observed, with stronger alignment of N400 peaks than onsets. The peak amplitude of the N400 effect correlates best with the latency characteristic showing less temporal dispersion. These findings suggest that meaning construction in the brain is subtly affected by task demands, and that there is complex functional integration between semantic combinatorics and control systems handling behavioral goals.

© 2012 Elsevier Ltd. All rights reserved.

1. Introduction

Language processing requires that representations of words are recovered from memory and unified in a temporary sentence structure. The interplay between lexical retrieval and unification may be constrained by a variety of factors, including how the resulting interpretation is used to negotiate or act upon the current situation. On the assumption that such constraints are accessible to experimental research, several questions can be raised as to the neural structures and processes that support, or are affected by, the generation of goals for action during language comprehension. One key issue is whether behavioral goals, here operationalized as different task demands, produce effects that propagate in a cascading manner, affecting similarly all consecutive stages of word processing, or whether they selectively tap into distinct neural mechanisms, leading to dissociable effects instead. Whereas cascading effects would suggest that behavioral goals impact unselectively on sentence processing, acting rather as an external force with no access to individual stages of the computation, dissociable effects would show there is selective interaction between aspects of linguistic combinatorics and control systems responsible for handling goals.

The present event-related potential (ERP) study is an attempt at disentangling these two possibilities.

The remainder of this introduction is organized as follows. Section 1.1 presents the N400 effect in ERPs as a candidate neurophysiological marker for investigating the effects of exogenous factors, such as task demands, on lexical retrieval and unification. Section 1.2 reviews earlier work on the experimental variables that may affect the N400 waveform characteristics, in particular onset and peak latencies as potential neural signatures of consecutive word processing stages. Section 1.3 introduces the aims, motivations and hypotheses of the present study, which are further developed and clarified in Section 1.4, where a functional-anatomical model of semantic unification is described and used to specify how behavioral goals could affect N400 latency characteristics.

1.1. The N400 effect in event-related potentials

Event-related potentials (ERPs) are a valuable tool for mapping the occurrence of stimulus-induced brain responses onto a cognitive processing timeline. The N400 component (Kutas & Hillyard, 1980) is a transient modulation of the electroencephalogram (EEG) that peaks at approximately 400 ms after the visual or auditory onset of a meaningful stimulus, such as a content word or a picture, and is largest over centro-parietal scalp sites. The N400 amplitude is inversely correlated ($r \approx -0.8$) with the degree of semantic fit

* Correspondence address: SISSA International School for Advanced Studies, via Bonomea 265, 34136 Trieste, Italy. Tel.: +39 040 3787602.
E-mail address: gbaggio@sissa.it

of the stimulus given the preceding context, for example a sentence (Kutas & Hillyard, 1984). The N400 effect – calculated as the time-resolved difference between N400 components in two experimental conditions, such as semantically or factually congruent and incongruent sentence types – provides information on the time course and difficulty of lexico-semantic processing (Hagoort, Baggio, & Willems, 2009; Kutas & Federmeier, 2000; Lau, Phillips, & Poeppel, 2008).

It has been noted (Federmeier & Laszlo, 2009; Kutas & Federmeier, 2011) that the N400 shows a stable peak latency, which appears to be largely insensitive to the experimental variables that typically modulate its amplitude. In seeming contrast with such claims, however, several studies reported or discussed variability in the N400 onset or peak time as a function of stimulus characteristics, task demands, sensory input modality (Deacon, Hewitt, & Tamny, 1998; Deacon, Mehta, Nousak, & Tinsley, 1995; Hagoort & Brown, 2000; Holcomb, 1988, 1993; Holcomb & Neville, 1990, 1991; Kutas, 1987; Marinkovic et al., 2003; O'Rourke & Holcomb, 2002; Vachon & Jolicoeur, 2011), and the cognitive and neurological conditions of participants (Ardal, Donald, Meuter, Muldrew, & Luce, 1990; Hagoort, Wassenaar, & Brown, 2003; Kutas & Iragui, 1998; Ruüsseler, Becker, Johannes, & Münte, 2007; Swaab, Brown, & Hagoort, 1997). A representative sample of those studies is reviewed below.

1.2. What factors affect N400 latencies?

1.2.1. Stimulus characteristics
Deacon et al. (1995) studied the consequences of priming on the timing of the N400 and of an earlier negativity labelled NA. The amplitude of the NA was not affected by priming, but the N400 effect was smaller for primed than for unprimed words. The authors performed current source density (CSD) analyses on the ERP data, which showed the activation of multiple neural generators in the N400 interval. Deacon et al. claimed that ERPs and CSDs are "consistent with the existence of two types of N400": a frontal N400 varying in latency as a function of semantic priming, and a posterior N400 that varies in amplitude. However, the authors did not discuss the possibility that the 'frontal N400' is a different ERP component altogether. They decided to take the earlier component to be an N400 because "participants were required to semantically categorize words" (Deacon et al., 1995, pp. 567–568). Therefore, the conclusion that the N400 latency varies as a function of priming appears to be unsupported. Similar concerns can be raised for other priming studies, such as Deacon et al. (1998).

1.2.2. Sensory modality
The first demonstration of N400 latency shifts can be found in Kutas (1987), who showed that the N400 effect was delayed when the interval between visually presented words was reduced to about 100 ms. Further studies provided evidence for small but reliable variations in the timing of the N400. For example, Holcomb and Neville (1990) administered a lexical decision task in the visual and auditory modalities. The stimuli were a prime word followed by a semantically related word, an unrelated word, or a non-word. As expected, N400s were larger to unrelated words than to related words in both modalities. However, the effect began earlier in the auditory than in the visual modality – see also Holcomb and Neville (1991) for a study on related topics.

Hagoort and Brown (2000) raised the issue of whether the latency shifts reported by previous research are genuine modulations of the N400 onset, or whether they are instead a manifestation of a different effect, preceding the N400 in time. The authors presented ERP data suggesting that the N400 in response to speech is indeed introduced by an early negativity: the N250. The N250 and N400 in this study had similar topographic characteristics, but they could be disentangled given the different time frames at which the components showed relative maxima: around 250 and 400 ms respectively. In a subsequent study, van den Brink, Hagoort, and Brown (2001) reported ERP effects earlier than the N400, elicited by words that were incongruent given the sentence context, and whose initial phonological characteristics differed from those of congruent completions. These experiments indicate that differences in lexical processing between the auditory and the visual modalities may affect the amplitude of earlier ERP components (N200 or N250), rather than the onset of the N400 effect.

1.2.3. Special populations
Kutas and Iragui (1998) reported a decrease in N400 amplitudes and an increase in peak latencies as the age of participants increased. Moreover, the N400 component peaked later in bilinguals: monolinguals had the shortest N400 latency, followed by the first language of bilinguals, and by the second language of bilinguals last (Ardal et al., 1990; Moreno & Kutas, 2005). The peak latency of the N400 appears to be delayed in late bilinguals too (Weber-Fox & Neville, 1996). In agrammatic patients, the onset of the N400 effect was slightly later than in normal populations (Hagoort et al., 2003; Swaab et al., 1997), and the same applies to dyslexic readers (Ruüsseler et al., 2007). These findings suggest that the less comparable two groups – the more different in age, in linguistic experience or in neurological condition – the larger the differences between groups in N400 amplitudes or latencies.

1.2.4. Task demands
Holcomb (1988) investigated semantic priming in lexical decision tasks. In one block of trials, the instructions and item distribution induced participants to process primes automatically, whereas in another block participants were asked to attend to the meaning of the prime. Interestingly, the N400 effect – the difference between neutral and related primes – was somewhat earlier in the attentional than in the automatic block. Holcomb did not use a systematic procedure to quantify such onset latency differences. Rather, he observed that the grand-average difference wave in the attentional block "crossed the zero baseline at 180 ms and was clearly negative at 210 ms, while the automatic block difference wave crossed baseline at 210 ms and did not go substantially negative until 270 ms". Holcomb argued that "although any firm conclusion must await a more controlled chronometric study of the N400 onset times these data do suggest that paying attention to the meaning of the prime enhanced some aspect of the encoding operations performed on the related targets" (Holcomb, 1988).

In recent work, Vachon and Jolicoeur (2011) showed that task demands can affect N400 latencies. They examined the N400 effect elicited by the second of two subsequent words presented visually, either in task-set switching or in no-switching conditions. The N400 was delayed and reduced in amplitude in the switching, but not in the no-switching condition, when the targets were adjacent in the sequence. In this experiment, N400 latency differences were inferred using a jackknife approach, where n grand average waveforms were computed with $n-1$ participants (a different participant was removed for each waveform), and latency onsets were estimated for each grand-average wave. The estimates were obtained for different time intervals in the switch and no-switch conditions, and were contrasted using paired-sample T tests.

Despite the differences between the informal approach of Holcomb and the statistical procedure of Vachon & Jolicoeur in how N400 onset latency differences were identified, the studies involving task manipulations just reviewed showed no evidence of contamination of N400s by earlier negative (N200 or N250) or positive (P300) components.
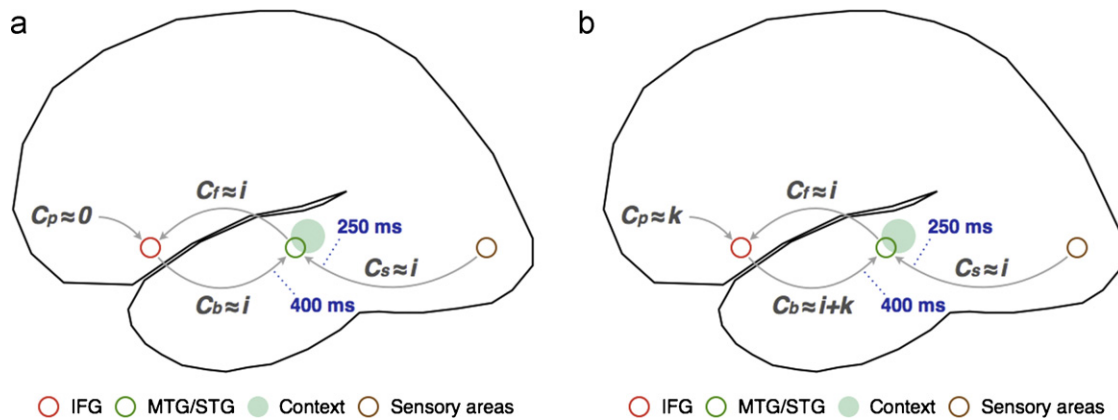
Fig. 1. Two applications of the cycle model by Baggio and Hagoort (2012). Word processing in context is subserved by a perisylvian network including the inferior frontal gyrus (IFG) and middle and superior temporal gyri (MTG/STG). Input currents (C_s) are conveyed from sensory areas to temporal cortex, where lexical information is activated. Currents are fed forward (C_f) to frontal cortex, and are relayed back (C_b) into the same temporal areas from where they were received. A recurrent network is thus set up, which allows information to be maintained on-line, a context to be constructed during successive processing cycles, and incoming words to be unified within the context. Additional currents may enter the cycle at different stages, such as through prefrontal regions (C_p) if additional contributions of control systems are required in the relevant behavioral setting: (a) shows how the input current i is transferred through the cycle when other inputs (e.g., C_p) are negligible; (b) shows the increase in feedback currents (C_b) following the application of an additional control input k. Details for these two cases are given in the main text. Blue labels show the approximate times at which currents reach temporal cortex during the forward and backward processing phases. (For interpretation of the references to color in this figure legend, the reader is referred to the web version of the article.)

1.3. The present study

The amplitude of the N400 is known to vary with stimulus characteristics, such as the degree of semantic fit between a word and the context in which it occurs. There is however limited evidence that similar kinds of experimental manipulations affect the N400 peak or onset latency, and that such effects are independent of amplitude differences and of modulations of earlier ERP components such as the N200 or the N250. This problem was encountered above while discussing N400 latency effects specific to different sensory modalities. ERP studies on special populations suggest that sufficiently large differences in N400 latencies may arise only between fairly heterogeneous groups, that may not be comparable in many respects. Although further research needs to be carried out involving the design variables mentioned above, taken together these studies indicate that task manipulations may be, given present knowledge, the most effective way to interfere with the onset latency of the N400 effect. Therefore, the N400 may be a valid testing ground for hypotheses bearing on the interplay between linguistic combinatorics and cognitive control as involved in setting behavioral goals for different tasks.

The motivation for the research reported here is threefold: first, to provide further evidence that task demands affect N400 onset latencies, along the lines of Holcomb (1988) and Vachon and Jolicoeur (2011); second, to determine whether a task manipulation leads to selective effects (affecting either N400 onset or peak latency, but not both) or to cascading effects (affecting N400 peak latency whenever onset latency is affected); third, to develop formal tools for analyzing onset and peak latency effects over whole ERP topographies (electrodes), rather than over trials or participants. The following section provides some arguments for the latter choice, as well as a theoretical framework in which N400 onset and peak latencies can be assigned an explicit functional-computational role.

1.4. Hypotheses from a model of the N400

Baggio and Hagoort (2011) propose a model in which the N400 is seen as reflecting a word-processing cycle, starting with the retrieval of lexical information and leading to the unification of the word's meaning into a discourse structure (Hagoort et al., 2009). The cycle model tries to overcome the opposition between retrieval-based and integration-based accounts of the N400. Indeed, a number of authors have pointed out that neither account is entirely consistent with all available N400 data (Baggio & Hagoort, 2011; Federmeier & Laszlo, 2009; Kutas & Federmeier, 2000, 2011) – in these articles the reader will find extensive literature coverage and detailed discussion. For example, retrieval-based accounts predict and explain N400 effects in paradigms where contextual expectancy is manipulated (Kutas & Federmeier, 2000; Lau et al., 2008), such as in the priming studies reviewed above. However, they cannot account for N400 effects elicited by words that require additional unification effort, and yet are not contextually unexpected or inappropriate with respect to their control counterparts (Baggio, Choma, van Lambalgen, & Hagoort, 2010; Kuperberg, Choi, Cohn, Paczynski, & Jackendoff, 2010; Li, Hagoort, & Yang, 2008). Conversely, integration-based theories can explain the latter kind of findings (Hagoort et al., 2009), but appear to be less suited to account for pre-activation or priming phenomena.

The cycle model describes in simple dynamic terms aspects of the functioning of the perisylvian language network. According to the model, the N400 is generated within this network in two coarsely-defined phases (Fig. 1). In phase one, currents from sensory pathways (C_s), such as the ventral visual stream in reading, reach middle and superior temporal gyri (MTG/STG) at approximately 250 ms from word onset (Marinkovic et al., 2003). This is a critical stage in the access and retrieval of lexical meanings, and marks the outset of the ascending phase of the N400. In phase two, currents from temporal regions flow forward (C_f) to the inferior frontal gyrus (IFG), and are relayed back (C_b) into the same areas in temporal cortex from where they were received. This sets up a recurrent circuit which affords persistent reverberating activity of the kind required to bind information over different time scales. Brain imaging data suggesting the existence of a fronto-temporal cycle are provided by Tse et al. (2007).

In the cycle model, the onset of the N400 coincides with the first injection of currents into middle and superior temporal areas (250 ms), whereas the N400 peak results from the re-injection of currents into temporal regions (400 ms) following inferior frontal processing. The amplitude of the N400 is a function of the degree of overlap in temporal cortex between the neuronal populations recruited by the eliciting word (Fig. 1, empty green circle) and the

populations that encode a semantic context resulting from processing the preceding lexical material (Fig. 1, green shaded area). The cycle model accommodates both pre-activation, which is seen as a function of input-context population overlap, and integration, whereby a context, such as a sentence-level semantic representation, is progressively built up through the contribution of inferior frontal regions in successive word-processing cycles. As such, this model may be a first step toward bridging the divide between retrieval-based and integration-based accounts of the N400 – see Baggio and Hagoort (2011) for details.

The electromagnetic activity of cortical sources is typically not reflected in linearly-scaled voltage changes measured at the scalp locations that would be identified based on a radial source-to-scalp mapping. In particular, the left temporal source of the N400 (Halgren et al., 2002; Helenius, Salmelin, Service, & Connolly, 1998; Simos, Basile, & Papanicolaou, 1997) does not result in a focal left temporal scalp ERP, and by the same token phase one and phase two of the cycle model cannot be expected to produce frontal and temporal modulations of scalp ERPs. Moreover, turning from the spatial to the temporal domain, precise timing predictions – for example, of the time lag separating phase one and phase two – would require knowledge of conduction times between temporal and frontal cortex, which in turn would be based on detailed neuroanatomical and neurophysiological information that is currently not available using non-invasive methods. However, the N400 onset and peak latencies can be used to constrain, in the cycle model, the approximate timing of current injection into MTG/STG during phase one and phase two.

To make the cycle model predictive, one needs the additional hypothesis that, during the generation of the N400, currents are (re-)injected into temporal cortex in a single shot within a narrow time window, rather than gradually over a longer time frame, reflecting the tight deadlines imposed by direct white matter connections between sensory-motor, frontal and temporal regions – see Baggio and Hagoort (2011) for a discussion of the roles of connectivity and neurotransmitters on the timing of information flow in perisylvian cortex. If this is correct, phase one may be indexed by the temporal alignment of N400 onsets across different recording sites, reflecting the transfer of information from sensory to temporal regions in one compact wave. By the same logic, phase two should produce a topographic alignment of N400 peaks, reflecting the feeding-back of electrical potentials from frontal to temporal cortices in a similar time-constrained manner – see Damasio (1989), von der Malsburg (1995), Churchland et al. (2010) for discussions of the role of narrow time windows in neural information processing. Importantly – simplifying matters somewhat, for details see Luck (2005) – ERPs do not reflect action potentials produced by cortical neurons, but post-synaptic currents flowing from axons to the receiving neurons, where action potentials are then produced. This is consistent with the cycle model's proposal that the temporal alignment of N400 onsets and peaks reflects currents at the receiving end of long-distance cortical transmission. Studies that attempted a reconstruction of the cortical sources of the N400 (Halgren et al., 2002; Helenius et al., 1998; Simos et al., 1997) suggest that such receiving end may indeed be in temporal cortex.

The degree of N400 onset and peak alignment may depend on a variety of conditions, including behavioral goals. Consider the situation in which one is silently reading a text, such as a history book, with the sole purpose of understanding what is written. In that case, the sensory input currents i will be simply transferred within the cycle to temporal and frontal regions (Fig. 1a). Assuming that the contribution of control systems in silent reading is negligible ($C_p \approx 0$), and that there is no additional input to inferior frontal areas, it follows that $C_b \approx C_f$. Crucially, the sensory input C_s is then the largest single contribution to the neuronal generators of the N400 in temporal cortex. In such conditions, phase-one

processing would gain prominence in the generation of the N400. If the proposed single-shot information-transfer hypothesis is correct, this would result in a tighter alignment of N400 onsets across electrodes.

Consider now a different situation: one is silently reading a text, again a history book, with the purpose of retaining some of the written information to carry out a short-term task, such as remembering the name of a statesman to then search the web for a biographical sketch. In that case, C_s is no longer the only input to the cycle (Fig. 1b). A positive value for C_p would contribute to making $C_b > C_f$. Because $C_f \approx C_s$, it follows that $C_b > C_s$. Therefore, C_b will now be the largest single contribution to the generators of the N400 in temporal cortex. Here, phase-two processing would become more prominent, resulting in a tighter alignment of N400 peaks across electrodes.

Testing these predictions requires new mathematical tools for quantifying the temporal alignment of ERP latency characteristics across electrodes – an effort which is undertaken in the present paper. The different behavioral goals associated with reading in the history book example mentioned above will be operationalized as different experimental tasks, and will be used to decide whether (1) the more demanding task has cascading effects on consecutive word processing phases, affecting both onset and peak alignment or (2) the task has selective effects on consecutive word processing phases, leading to a dissociation of onset and peak alignment. The cycle model does not make predictions to this regard. Hence, new ERP data are necessary to integrate the model's architecture with a more precise view of the dependence between onset and peak latencies.

2. Methods

2.1. Participants

Forty eight right-handed native speakers of Dutch (30 females, mean age 22.25) took part in the experiment after giving written informed consent. Participants were undergraduate students of the Radboud University Nijmegen with normal or corrected-to-normal visual acuity, and no history of neurological or cognitive disorders. The study was approved by the local ethics committee.

2.2. Materials

The experimental stimuli were 80 sentence pairs in Dutch. Each pair contained a congruent sentence (e.g., 'Pine trees stay green throughout the year') and an incongruent sentence (e.g., 'Pine trees stay red throughout the year'). Congruency is here defined as consistency with world knowledge (Hagoort, Hald, Bastiaansen, & Petersson, 2004). Congruent and incongruent sentences within a pair differed in a single non-final critical word ('green'/'red'). Mean length, word form frequency and lemma frequency of critical words from the CELEX corpus for written Dutch (Baayen, Piepenbrock, & Gulikers, 1996) were matched across the two experimental conditions (T tests, $p > 0.1$ in all comparisons). Fillers were 160 sentences with varying content, syntax and length in number of words. Two lists of sentences were produced, each containing either the congruent or the incongruent sentence from each pair, and all fillers. Thus, in each list there were 40 congruent and 40 incongruent sentences, and 160 fillers. An equal number of participants was assigned to each list.

All sentences – experimental and filler – were presented one word at a time (300 ms on-screen duration of each word, 300 ms between-word blanks; viewing distance: 100 cm; visual angle: 3° horizontal, 0.5° vertical) and were preceded by a mini-discourse constituted by two sentences shown on a single screen, introducing the topic on which experimental and filler sentences would provide further comment. For experimental items, mini-discourses were exactly the same for both sentences in a pair. The last word of each sentence was marked by a full stop and was followed by a fixation cross lasting for 1500 ms on the screen. After each trial, participants would press any of two keys on a button box with their right index or middle finger to proceed to the next trial.

The initial sensory input (a sentence) and the final motor output (a button press) were the same for all 48 participants, in all trials. However, participants were assigned to two groups. While the EEG was recorded (see details below), 24 participants (13 females, mean age 22) were instructed to read silently each sentence for comprehension, with no additional task than to press a button to move on to the next trial. This will be referred to as the silent reading task group, abbreviated as SRT. The remaining 24 participants (17 females, average age 22.5) were similarly instructed to read each sentence silently. In addition, after each sentence, a pair of

Table 1
Summary of ANOVA statistics on ERP data ($N = 24 \times 2$ groups). The dependent variable is the mean amplitude of the N400 component (μV). p-Values smaller than $\alpha = 0.05$ are indicated with an asterisk.

Factor	DF	Sum of squares	Mean squares	F	p
Group	1	3656	3656.0	542.5468	0.0001*
Electrode	28	390	13.9	2.0665	0.0008*
Condition	1	641	641.2	95.1538	0.0001*
Interval	1	193	193.0	28.6358	0.0001*
Group × Electrode	28	1059	37.8	5.6114	0.0001*
Group × Condition	1	8	7.7	1.1424	0.2852
Electrode × Condition	28	117	4.2	0.6200	0.9408
Group × Interval	1	17	16.9	2.5032	0.1137
Electrode × Interval	28	247	8.8	1.3108	0.1264
Condition × Interval	1	21	20.7	3.0766	0.0795
Group × Electrode × Condition	28	52	1.9	0.2766	0.9999
Group × Electrode × Interval	28	49	1.8	0.2619	0.9999
Group × Condition × Interval	1	7	7.1	1.0517	0.3052
Electrode × Condition × Interval	28	31	1.1	0.1651	0.9999
Group × Electrode × Condition × Interval	28	9	0.3	0.0489	1.0000
Residuals	5220	35176	6.7		

probes ('The color of pine trees is always green', 'The color of pine trees is always red') was shown in separate rows on a single screen. Using the button box, participants from the second group had to select the probe that matched in content the previous sentence. This will be referred to as the probe selection task group, abbreviated as PST. The position of the matching and mismatching probes on the screen (top or bottom) was randomized and counterbalanced in each stimulus list. The experiment was divided into 24 blocks of 10 trials.

2.3. Data acquisition

The EEG was sampled at 500 Hz using a BrainAmp DC system with a 125 Hz low-pass filter, a 10 s time constant, and no notch filter, from 28 scalp locations: Fp1, Fp2, F7, F3, Fz, F4, F8, FC5, FC1, FCz, FC2, FC6, T7, C3, Cz, C4, T8, CP5, CP1, CP2, CP6, P7, P3, Pz, P4, P8, O1 and O2. Three electrodes, one below the left eye and two near each outer canthus, were used to record the EOG. One electrode on the left mastoid bone (TP9) served as reference during the measurement. The EEG and EOG were re-referenced off-line to a linked mastoid reference using signals from a right mastoid channel (TP10).

2.4. Data analysis

Epochs were extracted from the EEG in the interval [−200 600] ms relative to the visual onset (0 ms) of critical words.[1] Baseline-correction used the average amplitude value in the interval [−200 0] ms relative to the onset of critical words. Epochs were discarded if they contained activity exceeding ±100 μV thresholds in any EEG channel. Eye movements or blinks in the EOG channels were identified by means of the following procedure: (1) EOG data were filtered at 1–15 Hz; (2) Hilbert analytic amplitudes were computed, resulting in the envelope of each EOG signal; (3) envelopes were normalized calculating z scores for each EOG channel; (4) one z value per time point was computed, summing the z scores from each EOG channel and normalizing the sum by dividing it by the root of the number of EOG channels; (5) EOG segments exceeding the resulting threshold were discarded. Artifact rejection did not involve visual inspection of the data, and was entirely automatic.

ERPs for each participant were computed by averaging over artifact-free epochs belonging to each experimental condition, and grand-average ERPs were derived by further averaging over participant-specific averages. A mixed ANOVA model with 4 factors was used to analyze ERP data (Table 1): Group (between participants, 2 levels: SRT/PST), Electrode (29 levels: Fp1 to O2, plus TP10), Condition (2 levels: congruent/incongruent), and Interval (2 levels: ascending/descending phases of the N400 effect; 324–368 ms and 368–552 ms in the SRT group; 234–392 ms and 392–540 ms in the PST group; Fig. 2d and h; details on the computation of these time windows are given hereafter). The dependent variable in the ANOVA was the mean amplitude of the N400 (μV).

A non-parametric statistical procedure was used to characterize, in each group, the temporal profile of the N400 effect. For mathematical details, the reader is referred to Maris and Oostenveld (2007).[2] Participant-specific ERP averages from the two conditions were collected in a single set, which was then randomly partitioned into two subsets of equal size. The means of the subsets were compared using

a dependent-samples T test. By repeating these two steps 10,000 times, a p value was estimated as the proportion of random partitions resulting in a larger T statistic than in the observed distribution. The null hypothesis that the ERP waveforms in the two experimental conditions are exchangeable is rejected if p is smaller than $\alpha = 0.05$.

To identify the spatio-temporal loci in which the conditions differ, ERP averages were compared using a T test in each electrode-time pair. The pairs (also called 'samples') whose T values exceeded the 95th quantile of a T distribution were used to construct spatio-temporally connected sets. For the present 28-channels array, organized according to the 10–20 system, neighborhood geometry was defined as follows: the electrodes in the array E are adjacent if and only if the paths connecting each and every other e in E never cross. The cluster-level T statistic (T_{sum}) is the sum of T values over the samples within a spatio-temporally connected set (a 'cluster').

To estimate the latency of N400 onsets and investigate their temporal alignment across electrodes, the following procedure was applied. Based on the output of non-parametric statistics, *inclusion matrices* of binary values (0, 1) were constructed – here matrix size is 28×400, where rows are electrodes and columns time points – specifying, for each electrode-time pair, whether the test statistic in the given sample is associated with a $p < \alpha$ (the corresponding element in the inclusion matrix is 1) or not (0). A sum over the rows of an inclusion matrix yields a *count vector* of 400 elements, representing, for each element (a data point, one every 2 ms), the number of electrodes in which $p < \alpha$.

The onset of the N400 effect was derived from non-parametric statistics as the first point in time of an uninterrupted sequence of non-zero elements in a count vector. The N400 onset was also estimated for each electrode separately, searching each row e of the inclusion matrix **M** for the first data point t at which $m_{e,t} = 1$. The onset t is the earliest point at which the N400 effect is significant over electrode e. A constraint on the search is imposed: that $t \geq k$, where k is the onset of the statistical N400 derived from the count vector. A count vector specifies the onset of the statistical N400 (sN400), whereas the inclusion matrix establishes, for each recording site, the latency point at which the N400 effect emerges. The amplitude and the latency of the N400 peak coincide with the minimum of the raw effect (i.e., the maximum negative amplitude of the N400, computed as the difference between waveforms in the two experimental conditions) in each electrode, and the time at which such minimum occurs, respectively.

The analysis described above produced four vectors of 28 elements, each representing the onset or peak times of the N400 in the SRT or PST groups. Two more 28-cell vectors specified mean peak amplitudes at each electrode, for each group. To quantify the alignment of the elements in a vector, that is, how temporally close N400 onset or peak latencies are across recording sites, the sum of pairwise Euclidean distances (SED) was computed between each x_i and every other x_j of n elements in vector X:

$$SED(x_i) = \sum_{j=1}^{n} |x_i - x_j| \tag{1}$$

This procedure transforms a vector X into its distance image $DI(X)$, where each element x_i of X is projected onto its sum of Euclidean distances $SED(x_i)$ in $DI(X)$. The sum of Euclidean distances is used here as a misalignment index: the higher SED, the more temporal dispersion there is across onset (or peak) times. The measures just described produce non-normal data distributions ($p < a' = 0.0063$ for onset and peak latency topographies and SED vectors; Shapiro–Wilk normality tests). Accordingly, the data were analyzed using non-parametric Wilcoxon signed rank tests instead of T tests (Table 2).

---

[1] Data analyses were carried out using FieldTrip (Oostenveld, Fries, Maris, & Schoffelen, 2011) (http://fieldtrip.fcdonders.nl/), a MATLAB toolbox developed at the Donders Institute for Brain, Cognition and Behaviour.

[2] For MATLAB tutorials, see: http://fieldtrip.fcdonders.nl/tutorial/.

Table 2
Summary of Wilcoxon signed rank tests on N400 topographies ($N = 28$). Bonferroni-corrected $\alpha' = 0.0071$. p-Values smaller than α' are indicated with an asterisk. SED is the sum of Euclidean distances.

Test	Measure	Comparison	Mean values (SD)	DF	V-value	p-Value
a	Onset latency	SRT/PST	336.21(14.56)/294(78.93)	28	314	0.0028 *
b	Peak latency	SRT/PST	393.21(26.62)/393.79(19.66)	28	106	0.5870
c	Peak amplitude	SRT/PST	−2.5437(0.75)/− 2.2082(0.88)	28	78	0.0034 *
d	SED	Onset: SRT/PST	348.43(264.79)/2035.71(1398.56)	28	0	0.0001 *
e	SED	Peak: SRT/PST	798.71(319.86)/516.14(332.96)	28	349	0.0009 *
f	SED	SRT: onset/peak	348.43(264.79)/798.71(319.86)	28	26	0.0001 *
g	SED	PST: onset/peak	2035.71(1398.56)/516.14(332.96)	28	406	0.0001 *

To determine whether the alignment of N400 onsets or peaks across electrodes, as revealed by the SED method, is modulated by ERP components that are statistically independent from the N400, three data decomposition procedures were applied to EEG epochs from the two experimental conditions: (1) fast independent component analysis based on Hyvärinen's (1999) fixed-point algorithm (henceforth 'fast ICA'); (2) Bell and Sejnowski's logistic infomax independent component analysis algorithm (Makeig, Bell, Jung, & Sejnowski, 1996) (henceforth 'ICA'); (3) principal component analysis (PCA). All three procedures used the standard computing routines available in FieldTrip and other MATLAB packages for EEG data analysis. Mean amplitudes of independent and principal components in the congruent and the incongruent conditions in two relevant time windows (details in Section 3) were statistically analyzed using non-parametric Wilcoxon signed rank tests (Table 4).

3. Results

3.1. Behavioral responses

Button-press responses in the PST (probe selection task) group show that the probes were correctly selected in 98.6% of trials on average for congruent sentences, and in 92.8% of trials on average for incongruent sentences ($T(24) = 5.3415$, $p < 0.001$). Matching the probes to experimental sentences took longer in the congruent (1.89 s, SD = 0.64 s) than in the incongruent condition (1.82 s, SD = 0.63 s; $T(24) = 2.1811$, $p = 0.039$). In the SRT (silent reading task) group, there was no difference in the frequency of button-presses with the index finger (M = 42.25, SD = 12.8) and the middle finger (M = 37.75, SD = 12.8; $T(23) = 0.861$, $p = 0.398$; paired-samples T test).

3.2. Event-related potentials

The N400 effect is comparable in the two groups (Fig. 2), as is indicated by the absence of an ANOVA interaction between Group and Condition (Table 1). However, the cluster-based non-parametric procedure reveals some differences in the strength as well as in the extent of the N400 effect: $T(24)_{sum} = -5236.2$,
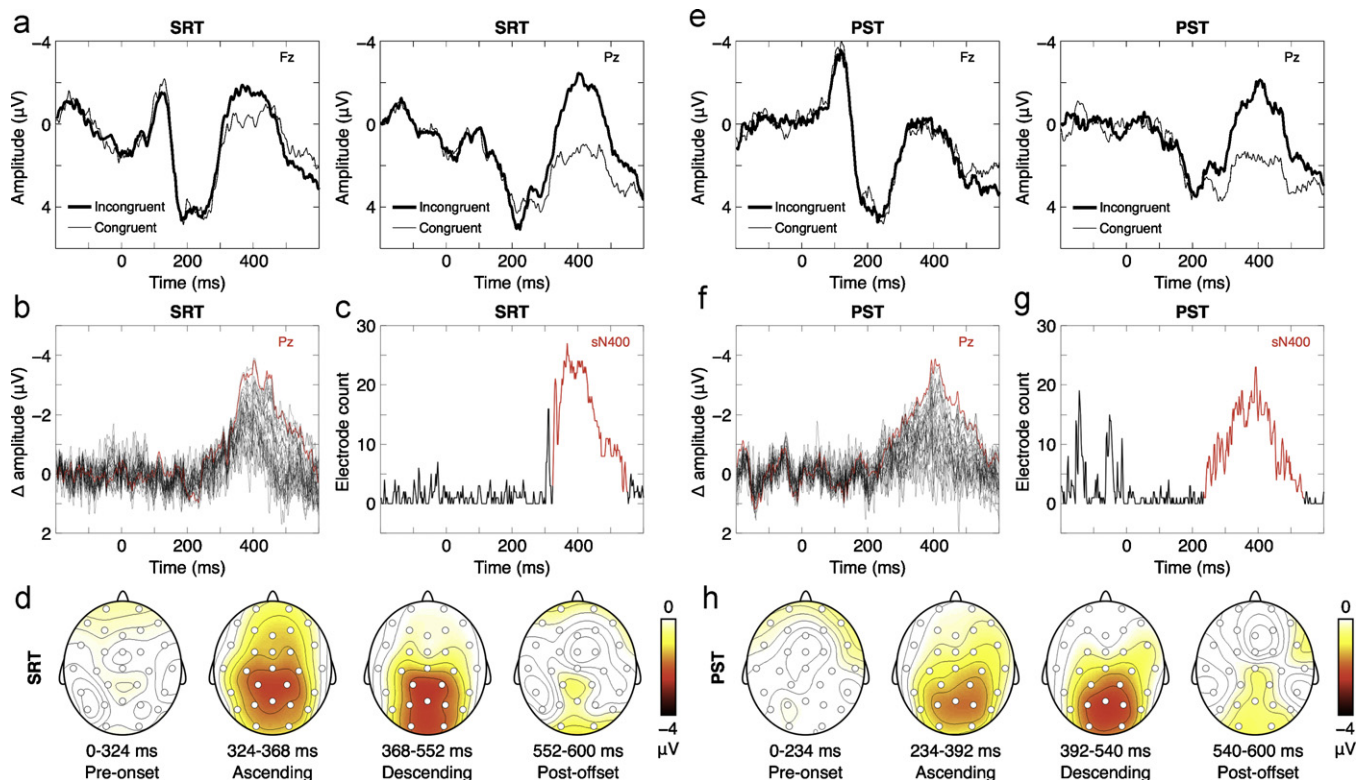

Fig. 2. (a) Grand-average ERP waveforms ($N = 24$) from a frontal (Fz) and a parietal (Pz) midline electrodes, time-locked to the onset (at 0 ms) of the critical word in the SRT (silent reading task) group. (b) N400 effect in the SRT group. Critical word onset is at 0 ms. Each waveform shows the N400 effect (incongruent minus congruent condition) from a different electrode. The effect is largest at the parietal midline site Pz, highlighted in red. (c) Number of electrodes at which the N400 effect is significant as a function of time in the SRT group. The count vector was obtained from non-parametric cluster-based randomization statistics (see Section 2). The statistical N400 effect (sN400), defined as an uninterrupted sequence of non-empty clusters of electrodes in which the conditions differ, is highlighted in red. The onset, peak and offset latencies were used to produce the topographic maps in (d), showing pre-onset, ascending, descending and post-offset phases of the N400 effect (mean difference between conditions in each time window). Panels (e–h) show the corresponding results for the PST (probe selection task) group ($N = 24$). (For interpretation of the references to color in this figure legend, the reader is referred to the web version of the article.)

$p < 0.0001$, $S = 1512$ in the SRT group and $T(24)_{sum} = -3449.9$, $p = 0.009$, $S = 1142$ in the PST group; S is the sum of the spatio-temporally connected samples (electrode-time pairs) in which waveforms are significantly different.

As detailed in Section 2, the iterated sample-based test statistic generates a matrix of binary values (0, 1) specifying, for each electrode (matrix rows), whether the N400 is significant at a particular time point (matrix columns). The sum over the rows of an inclusion matrix yields a count vector in which each element is the number of electrodes per time point showing a reliable difference in ERP amplitudes. Count vector estimates show that the N400 onset latency is later in the SRT group (324 ms, Fig. 2c) than in the PST group (234 ms, Fig. 2g). Based on inclusion matrices, N400 onset latencies can be calculated for each channel separately, resulting in average onsets at 336.21 ms (SD = 14.56) in SRT and 294 ms (SD = 78.93) in PST. The seeming discrepancy in N400 onset latencies in the PST group between count vector (234 ms) and inclusion matrix (294 ms) estimates is due to the fact that the latter is an *average* over electrode-specific onsets which show considerable temporal dispersion (e.g., SD = 78.93). Note however that there is no opposition between the two methods (count vectors are derived from inclusion matrices) unless average values are computed. These may be informative but, as is shown below, they rather conceal temporal variability in the data which may have some functional import. The difference between groups in mean onset latencies across recording sites is significant (Table 2a). The contrast in the N400 onset latencies between SRT and PST is shown in Fig. 3, which illustrates the different temporal evolution of the ascending phase (onset-to-peak) of the N400 in the two groups. There is no difference between groups in N400 peak latencies (Table 2b). However, there is a difference in mean peak amplitudes (Table 2c).

The statistical profile of the N400 in the SRT group (Fig. 2c) shows an early significant cluster of up to 16 electrodes, which returns to zero for two successive time frames (320–324 ms). Given the constraint of uninterrupted effects (see Section 2), that cluster was excluded from further data analyses. A post hoc search including the initial unconnected cluster yields a 304 ms count vector estimate of the N400 onset and a 322.14 ms (SD = 21.79) average over recording sites based on the inclusion matrix. Although the statistical onset of the N400 effect occurs considerably earlier in PST (at 234 ms) than in SRT (324 ms excluding the pre-interruption cluster vs. 304 ms including it), the average onset across electrodes is closest between PST (294 ms) and SRT (322.14 ms) when the estimate is based on the initially-excluded cluster. This is the result of introducing a tolerance factor in an otherwise objective procedure, and as such will not be pursued here. However, it will be shown below that the key finding of this study is not affected by considering onset estimates that include the disconnected SRT cluster.

Single-valued measures of spread around the mean provide some insight into the variability of a data set. In the present case, standard deviations are larger for onset latencies in PST than in SRT (Table 2a), whereas the reverse applies to peak latencies (Table 2b). This pattern is confirmed by observing inclusion matrices and N400 effect peaks. The alignment of onsets appears to be more consistent in the SRT (Fig. 4a) than in the PST group (Fig. 4e), whereas peaks are better aligned in PST (Fig. 4f) than in SRT (Fig. 4b). Temporal alignment was quantified by means of the sum of Euclidean distances (SED) between onset (or peak) latency in one electrode and onset (or peak) latency in every other electrode (see Section 2). SED is an index of misalignment of elements in a vector: the greater the dispersion of values, the larger the sum of distances. The SED analysis indicates that onset times are better temporally aligned in SRT (Table 2d), and peaks are better aligned in PST (Table 2e). In the SRT group onsets show greater alignment than peaks (Fig. 4c and Table 2f), whereas in the PST group peaks show greater alignment than onsets (Fig. 4g and Table 2g). Considering

Table 3
Summary of correlation tests on N400 topographies ($N = 28$). Bonferroni-corrected $\alpha' = 0.0083$ and $DF = 26$. p-Values smaller than α' are indicated with an asterisk.

Test	Variables	Pearson's correlations	Spearman's correlations
SRT			
a	Onset latency/peak latency	$T = 0.3521$	$S = 2734.068$
		$p = 0.7276$	$p = 0.1962$
		$r = 0.07$	$\rho = 0.25$
b	Onset latency/peak amplitude	$T = 4.3243$	$S = 2071.681$
		$p = 0.0002*$	$p = 0.0214$
		$r = 0.65$	$\rho = 0.43$
c	Peak latency/peak amplitude	$T = -1.8468$	$S = 4856.243$
		$p = 0.0762$	$p = 0.0873$
		$r = -0.34$	$\rho = -0.33$
PST			
d	Onset latency/peak latency	$T = 0.86$	$S = 2889.838$
		$p = 0.3976$	$p = 0.2855$
		$r = 0.17$	$\rho = 0.21$
e	Onset latency/peak amplitude	$T = 1.6937$	$S = 3711.110$
		$p = 0.1023$	$p = 0.937$
		$r = 0.32$	$\rho = -0.02$
f	Peak latency/peak amplitude	$T = -4.0411$	$S = 6045.817$
		$p = 0.0004*$	$p = 0.0002*$
		$r = -0.62$	$\rho = -0.65$

the disconnected cluster in the SRT group (Fig. 2c, recall the discussion above), the sum of Euclidean distances for onsets is larger: 580.86 ms, as compared to 348.43 ms reported in Table 2d and f and shown in Fig. 4c. However, this still gives a significant effect comparing SEDs of onset and peak times in the SRT group: $V(28) = 76.5$, $p = 0.0041$, instead of the V and p values in Table 2f. Moreover, onsets remain better aligned in SRT than in PST: $V(28) = 406$, $p = 0.0001$. The main result of this study – a double dissociation of onset and peak alignment depending on the task – is therefore stable regardless of whether or not N400 onset estimates are based on the initial detached cluster. Finally, in each group the amplitude of the N400 effect correlates best with the latency characteristic that shows less temporal dispersion – that is, with onset times in the SRT group (Fig. 4d and Table 3a–c), and with peak times in PST (Fig. 4h and Table 3d–f).

The N400 is best characterized as a complex neurophysiological response, with sources distributed over different regions of the cortex, giving rise to a number of independent evoked components, each of which contributes to the variability of the observed N400 waveform (Pylkkänen & Marantz, 2003). Three independent and principal component analyses (ICA and PCA) were carried out to determine whether the differences in N400 amplitude observed around peak and, in particular, onset times, are due to modulations of underlying ERP components occurring in the time intervals of interest and statistically separable from the main N400 response. The independent and the principal components that account for most of the variance (86–94%) were analyzed in two temporal frames: (1) an interval comprised between the onset of the N400 in the SRT group and the onset of the N400 in the PST group (234–324 ms), to detect any modulation of ERP components that would account for N400 onset differences between groups and (2) a window centered on the N400 peak (350–450 ms). Fast ICA revealed a single independent component (IC1, Fig. 5a and d), which however does not differ in amplitude in either time window and in either group (Table 4, Fast IC1). The same applies to the two next-in-rank components, sorted in descending order of mean projected variance (Table 4, Fast IC2-3). Fast ICA failed to
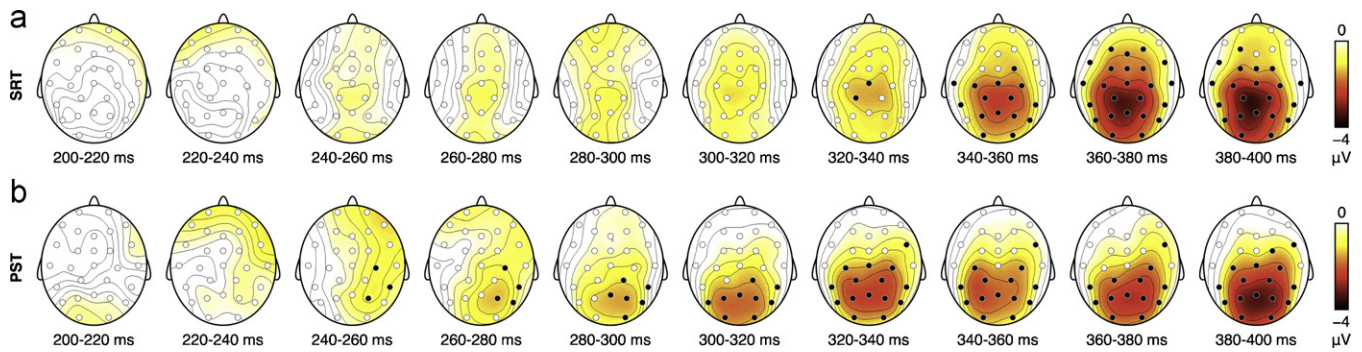
Fig. 3. (a) Topographic maps showing the temporal evolution of the ascending phase of the N400 effect (mean difference between incongruent and congruent condition) in time bins of 20 ms (10 data points) from 200 to 400 ms in the SRT (silent reading task) group ($N = 24$). Black circles represent the electrodes at which the N400 effect was significant ($p < \alpha = 0.05$, cluster-based randomization statistics) in at least 8 data points in each time bin, as specified by inclusion matrices (see Section 2; Fig. 4a and e). Panel (b) shows the corresponding result for the PST group ($N = 24$).

reveal any independent component that accounts for the observed N400 amplitude differences. As a consequence, the more standard logistic infomax ICA algorithm was also used, resulting in a decomposition of ERPs in three main independent signals, of which IC3 (highlighted in red in Fig. 5b and e) is the only one that differs in amplitude in the 350–450 ms frame in both groups (Table 4). Therefore, IC3 crucially contributes to the observed variation in N400 amplitude across conditions. A similar conclusion holds for the highest-ranked principal component, PC1 (Fig. 5c), which shows a significant amplitude difference between the conditions in the 350–450 ms window in the SRT group, and is reliably different in the same interval in the PST group (Table 4, PC1). Most importantly, the largest effects, though only approaching significance in

the 234–324 ms interval, are found for the independent component whose amplitude is modulated around the N400 maxima, namely IC3. This lends some support to the notion that the signal responsible for peak amplitude variations also contributes to onset latency variation. However, this is not to say that IC3/N400 is, in some relevant sense, a unitary physiological phenomenon. Quite the contrary, the dissociation in onset and peak latencies by task demands reported above suggests that this is not the case. Finally, these data speak against an alternative account of the observed onset latency differences in terms of components other than the N400, such as the N200 or the N250: fast ICA, ICA and PCA provide no evidence, in either group, for an earlier negative shift that is independent of the N400 and significantly different between conditions.
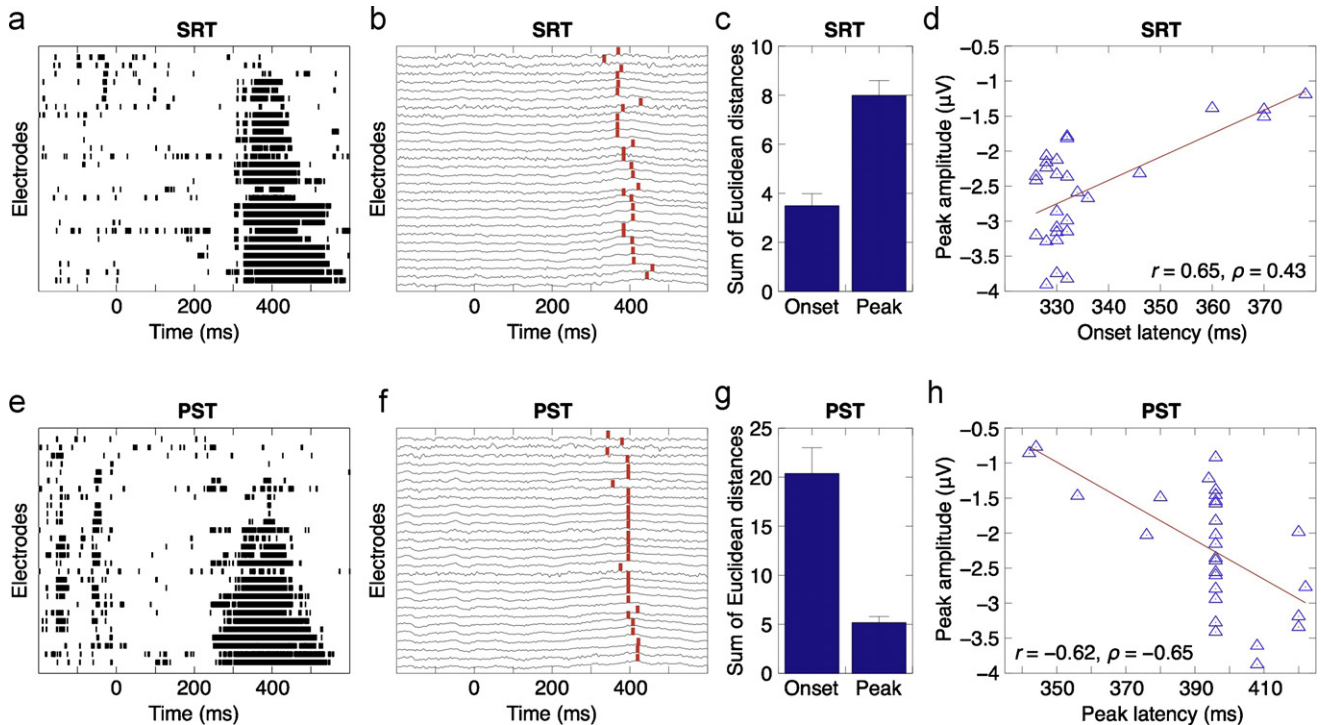

Fig. 4. (a) Raster plot of the binary inclusion matrix from non-parametric cluster-based randomization statistics for the N400 effect in the SRT (silent reading task) group. Each tick indicates that the ERP amplitude difference between conditions is significant at a particular electrode and point in time. (b) Waveforms of the N400 effect at each recording site are overlaid with a red tick representing the N400 peak, defined as the maximum negative amplitude value following the onset of the N400 effect at each electrode in the SRT group. (c) Bar chart of the mean of the sum of Euclidean distances (SED in 10^2 ms) between each and every other data point in a vector, representing the peak (or onset) times of the N400 effect at each electrode in the SRT group. Whisker length represents the standard error of the mean. (d) Correlation between onset latency and peak amplitude in the SRT group. Triangles represent electrodes ($N = 28$). Panels (e–g) show the corresponding results for the PST (probe selection task) group and (h) is the correlation between peak latency and peak amplitude in the PST group. (For interpretation of the references to color in this figure legend, the reader is referred to the web version of the article.)

Table 4
Summary of Wilcoxon signed rank tests contrasting mean component amplitudes ($N = 24$) in the congruent and in the incongruent conditions. Time intervals are given in milliseconds. Bonferroni-corrected $\alpha' = 0.0014$ and $DF = 24$. p-Values smaller than α' are marked with an asterisk.

Group	Component	Time	V	p	Group	Component	Time	V	p
SRT	Fast IC1	234–324	85	0.0653	PST	Fast IC1	234–324	228	0.0249
	Fast IC2	234–324	164	0.6997		Fast IC2	234–324	204	0.1280
	Fast IC3	234–324	187	0.2970		Fast IC3	234–324	114	0.3165
	IC1	234–324	162	0.7425		IC1	234–324	179	0.4155
	IC2	234–324	96	0.1263		IC2	234–324	99	0.1490
	IC3	234–324	75	0.0333		IC3	234–324	91	0.0946
	PC1	234–324	140	0.7860		PC1	234–324	110	0.2591
	PC2	234–324	101	0.1658		PC2	234–324	140	0.7861
	PC3	234–324	132	0.6170		PC3	234–324	139	0.7642
SRT	Fast IC1	350–450	181	0.3835	PST	Fast IC1	350–450	106	0.2182
	Fast IC2	350–450	141	0.8081		Fast IC2	350–450	152	0.9664
	Fast IC3	350–450	178	0.4320		Fast IC3	350–450	179	0.4223
	IC1	350–450	214	0.0696		IC1	350–450	196	0.1936
	IC2	350–450	217	0.0574		IC2	350–450	211	0.0839
	IC3	350–450	288	0.0001*		IC3	350–450	277	0.0003*
	PC1	350–450	13	0.0001*		PC1	350–450	49	0.0041
	PC2	350–450	102	0.1743		PC2	350–450	121	0.4155
	PC3	350–450	217	0.0574		PC3	350–450	222	0.0411

4. Discussion

Despite a wealth of ERP data, detailed functional accounts of the N400 are only starting to emerge (Federmeier & Laszlo, 2009; Kutas & Federmeier, 2011; Lau et al., 2008), none of which, however, seems capable of answering what controls the temporal profile of the N400. Moreover, none of the variables affecting the N400 amplitude (word repetition, word frequency, orthographic neighborhood density, semantic priming, contextual expectancy, plausibility, etc.) also affect onset or peak latencies. The temporal stability of the N400 peak has been recently emphasized (Federmeier & Laszlo, 2009; Kutas & Federmeier, 2011) in the context of theories proposing a limited time window for retrieving and integrating distributed multi-modal information in perceptual
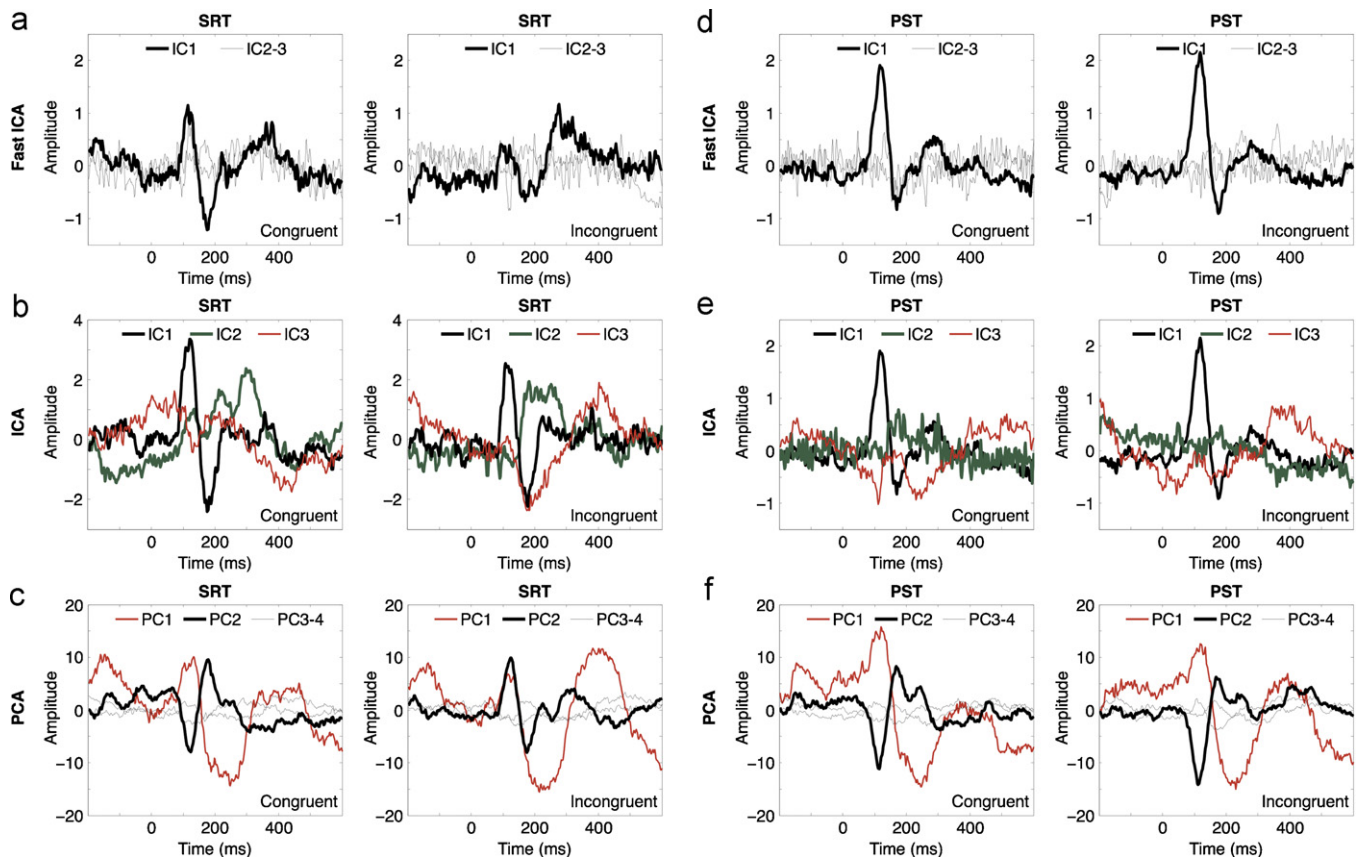

Fig. 5. (a) Fast independent component analysis (fast ICA) in the congruent (left) and incongruent (right) conditions, time-locked to the onset (at 0 ms) of the critical word in the SRT (silent reading task) group ($N = 24$). The highest-ranked independent component (IC1) is shown alongside two lower-ranked components, ordered by decreasing mean projected variance. (b) Independent component analysis (ICA). The three components that account for most of the variance are shown. See Section 2 for details on the difference between fast ICA and ICA. (c) Principal component analysis (PCA). The components that account for most of the variance (PC1 and PC2) are shown alongside two lower-ranked components (PC3 and PC4). Panels (d–f) show the corresponding results for the PST (probe selection task) group ($N = 24$). The waveforms shown in this figure are component time courses, invariant across recording sites. Activations are shown in arbitrary amplitude units that do not correspond to microvolt.

and memory processing (Damasio, 1989; von der Malsburg, 1995). The findings presented here suggest that this explanatory scheme needs to be enriched with hypotheses that explicitly distinguish N400 onset from peak latencies, and that attribute a functional role to the topographic alignment of each latency characteristic.

The present study reports a double dissociation in the latency characteristics of the N400 depending on task demands. In a silent reading task N400 onsets are better aligned than peaks, whereas in a probe selection task peaks are better aligned than onsets. Moreover, the N400 amplitude correlates best with the latency characteristic showing less temporal dispersion. In what follows, two aspects of these results are discussed: first, the methodological decision to quantify the alignment of onsets and peaks over electrodes, rather than over participants; second, a functional account, at the cognitive and neurobiological levels, of the observed dissociation in onset and peak alignment induced by task demands.

An attempt was made to run a latency alignment analysis on individual participants' datasets. The noisy character of EEG data affects the statistical stability of potential effects in individual N400 averages, one consequence of this being the difficulty to obtain estimates of onset and peak latencies for all or a fixed relevant subset of recording sites in all participants. In the non-parametric approach adopted here, single trials (instead of individual averages) can legitimately be used in the randomization procedure for each participant (instead of at the group level) (Maris & Oostenveld, 2007). An inclusion matrix and a count vector for each participant are derived. However, there is no guarantee that there will be significant clusters involving every electrode, or the same subset across participants, and that the N400 will have an onset at each recording site, in contrast with what holds for group-level inclusion matrices. On average, 15.88 (SD = 6.95) electrodes per participant show no statistical N400 onset in the SRT group, and 2.91 (SD = 3.75) in PST. Group-level overlap of sites showing N400 onsets is 0 in SRT, and 5 in PST. Any vector can be mapped to its distance image (see Section 2), but average SEDs cannot be sensibly compared for arrays of different length, and whose elements refer to different recording sites. This makes it a challenging task to determine, for individual participants, the onset of the statistical N400 effect as opposed to, for instance, the time point at which the N400 effect reaches a certain fraction of its peak amplitude value (Kutas & Iragui, 1998), a figure which may be unrelated to the time at which the effect becomes statistically significant at the group level. The approach presented here builds upon the rich output of non-parametric randomization tests over topographical ERP distributions, resulting in objective statistical estimates of the onset latency of the N400, based on inclusion matrices and count vectors. The measures of temporal alignment used here are applied to group-level effects, and as such they reflect a genuine statistical regularity. However, population-level effects of SED variability cannot be quantified, as the available formal tools make it impossible in practice to estimate the temporal variability of onset or peak latencies across electrodes and participants simultaneously. This limits the kinds of inferences that can be drawn from the proposed data analysis. Further research might lead to the development of novel data de-noising procedures and statistical tools that address this problem.

The key contribution of the present experiment is a first insight into the fine temporal structure of the cortical dynamics underlying goal-dependent language processing: a greater alignment of N400 onsets than peaks is seen in a silent reading task, whereas exactly the reverse is found when a probe selection task is administered. This double dissociation points to complex interfacing between linguistic combinatorics and control systems, such that the temporal structure of lexical processing can be subtly modulated by task demands. The topographical alignment of N400 onsets in a silent reading task is consistent with the possibility that, following the 'magic moment of word recognition' (Kutas & Federmeier,

2011), lexical meanings are accessed and retrieved in a fast, switch-like large-scale neural event, rather than in a gradual fashion. Although this scenario is still conjectural, using the tools of non-linear dynamical systems theory, Baggio and Fonseca (2012) carried out an in-depth analysis of the SRT data set, providing evidence that the N400 onset marks the outbreak of a phase transition in brain activity. This is to be expected in the light of the cycle model, which implies that the system enters a different dynamic regime when moving from phase one to phase two, that is, when the sensory input enters the perisylvian cycle, and perceptual analysis gives way to conceptual-semantic processing.

The cycle model, with the add-on hypothesis of one-shot information transfer between distant cortical areas, seems capable of accounting for the present data set. The model predicts that, in the absence of an input other than sensory currents, the neuronal generators of the N400 in temporal cortex will be largely driven by the feed-forward sensory input delivered around 250 ms (Fig. 1a), which will produce a more marked alignment of N400 onsets. When an additional control input is present, the N400 generators will receive the largest set of currents in the feed-back phase around 400 ms (Fig. 1b), and this will result in a more marked alignment of N400 peaks. However, the cycle model does not license specific predictions as to whether the N400 onset and peak latencies are dependent, as in a cascading architecture where peak alignment would increase whenever onset alignment increases, or whether the two mechanisms are dissociable. For this reason, this study was framed as an attempt to disentangle these two possibilities. The present data set provides evidence for a double dissociation. The largest current set reaching the N400 generators in temporal cortex uniquely determines which latency characteristic will show greater alignment. It is unclear whether the retrieval-based and the integration-based approaches would be capable of accounting for these findings. Both theories are designed to explain variations in N400 amplitudes, and both pinpoint a single processing mechanism – retrieval or integration – that may underlie amplitude changes. As a result, neither theory makes predictions regarding onset or peak timing, let alone the alignment of onsets and peaks across recording sites. Moreover, in light of the cycle model, and given that this study demonstrates systematic correlations with the best-aligned latency feature, N400 amplitudes may be a consequence of single-shot information transfer to temporal cortex in different processing phases. Taken together, these are indications that the latency characteristics of the N400 are at least as important as its amplitude, and deserve to become part of current attempts at analyzing the phenomenological, neurophysiological and functional underpinnings of the N400.

In conclusion, interpreted in the light of the cycle model by Baggio and Hagoort (2011), the present results are compatible with the existence of a phased set of cortical computations, sensitive to several external and internal systems conditions, which together give rise to the N400. The measures of temporal alignment introduced here, adjusted to allow population-level inferences, may prove a useful tool for inferring aspects of the temporal organization of cognitive processing from neurophysiological data.

Acknowledgments

References

Ardal, S., Donald, M., Meuter, R., Muldrew, S., & Luce, M. (1990). Brain responses to semantic incongruity in bilinguals. *Brain and Language*, *39*, 187–205.

Baayen, R., Piepenbrock, R., & Gulikers, L. (1996). *CELEX2*. Philadelphia: Linguistic Data Consortium.

Baggio, G., & Fonseca, A. (2012). Complex dynamics of semantic memory access in reading. *Journal of the Royal Society Interface*, *9*, 328–338.

Baggio, G., & Hagoort, P. (2011). The balance between memory and unification in semantics: A dynamic account of the N400. *Language and Cognitive Processes*, *26*, 1338–1367.

Baggio, G., Choma, T., van Lambalgen, M., & Hagoort, P. (2010). Coercion and compositionality. *Journal of Cognitive Neuroscience*, *22*, 2131–2140.

Churchland, M., Yu, B., Cunningham, J., Sugrue, L., Cohen, M., Corrado, G., Newsome, W., Clark, A., Hosseini, P., Scott, B., Bradley, D., Smith, M., Kohn, A., Movshon, J., Armstrong, K., Moore, T., Chang, S., Snyder, L., Lisberger, S., Priebe, N., Finn, I., Ferster, D., Ryu, S., Santhanam, G., Sahani, M., & Shenoy, K. (2010). Stimulus onset quenches neural variability: A widespread cortical phenomenon. *Nature Neuroscience*, *13*, 369–378.

Damasio, A. (1989). The brain binds entities and events by multiregional activation from convergence zones. *Neural Computation*, *1*, 123–132.

Deacon, D., Hewitt, S., & Tamny, T. (1998). Event-related potential indices of semantic priming following an unrelated intervening item. *Cognitive Brain Research*, *6*, 219–225.

Deacon, D., Mehta, A., Nousak, J., & Tinsley, C. (1995). Variation in the latencies and amplitudes of N400 and NA as a function of semantic priming. *Psychophysiology*, *32*, 560–570.

Federmeier, K., & Laszlo, S. (2009). Time for meaning: Electrophysiology provides insights into the dynamics of representation and processing in semantic memory. In B. Ross (Ed.), *Psychology of learning and motivation* (pp. 1–44). Burlington: Academic Press.

Hagoort, P., & Brown, C. (2000). ERP effects of listening to speech: Semantic ERP effects. *Neuropsychologia*, *38*, 1518–1530.

Hagoort, P., Wassenaar, M., & Brown, C. (2003). Real-time semantic compensation in patients with agrammatic comprehension: Electrophysiological evidence for multiple-route plasticity. *Proceedings of the National Academy of Sciences*, *100*, 4340–4434.

Hagoort, P., Hald, L., Bastiaansen, M., & Petersson, K. M. (2004). Integration of word meaning and world knowledge in language comprehension. *Science*, *304*, 438–441.

Hagoort, P., Baggio, G., & Willems, R. (2009). Semantic unification. In M. Gazzaniga (Ed.), *The cognitive neurosciences* (4th Ed., Vol. 51, pp. 819–836). Cambridge, MA: MIT Press.

Halgren, E., Dhond, R., Christensen, N., Van Petten, C., Marinkovic, K., Lewine, J., & Dale, A. (2002). N400-like MEG responses modulated by semantic context, word frequency, and lexical class in sentences. *NeuroImage*, *17*, 1101–1116.

Helenius, P., Salmelin, R., Service, E., & Connolly, J. (1998). Distinct time courses of word and context comprehension in the left temporal cortex. *Brain*, *121*, 1133–1142.

Holcomb, P. (1988). Automatic and attentional processing: An event-related brain potential analysis of semantic priming. *Brain and Language*, *35*, 66–85.

Holcomb, P. (1993). Semantic priming and stimulus degradation: Implications for the role of the N400 in language processing. *Psychophysiology*, *30*, 47–61.

Holcomb, P., & Neville, H. (1990). Auditory and visual semantic priming in lexical decision: A comparison using event-related brain potentials. *Language and Cognitive Processes*, *5*, 281–312.

Holcomb, P., & Neville, H. (1991). Natural speech processing: An analysis using event-related brain potentials. *Psychobiology*, *19*, 286–300.

Hyvärinen, A. (1999). Fast and robust fixed-point algorithms for independent component analysis. *IEEE Transactions on Neural Networks*, *10*, 626–634.

Kuperberg, G. R., Choi, A., Cohn, N., Paczynski, M., & Jackendoff, R. (2010). Electrophysiological correlates of complement coercion. *Journal of Cognitive Neuroscience*, *22*, 2685–2701.

Kutas, M. (1987). Event-related brain potentials ERPs elicited during rapid serial visual presentation of congruous and incongruous sentences. In R. Johnson, J. Rohrbaugh, & R. Parasuraman (Eds.), *Current trends in event-related potential research*. Elsevier Science: Baltimore.

Kutas, M., & Federmeier, K. (2000). Electrophysiology reveals semantic memory use in language comprehension. *Trends in Cognitive Sciences*, *4*, 463–470.

Kutas, M., & Federmeier, K. (2011). Thirty years and counting: Finding meaning in the N400 component of the event-related brain potential (ERP). *Annual Review of Psychology*, *62*, 14.1–14.27

Kutas, M., & Hillyard, S. (1980). Reading senseless sentences: Brain potentials reflect semantic incongruity. *Science*, *207*, 203–205.

Kutas, M., & Hillyard, S. (1984). Brain potentials during reading reflect word expectancy and semantic association. *Nature*, *307*, 161–163.

Kutas, M., & Iragui, V. (1998). The N400 in a semantic categorization task across 6 decades. *Electroencephalography and Clinical Neurophysiology*, *108*, 456–471.

Lau, E., Phillips, C., & Poeppel, D. (2008). A cortical network for semantics: (De)constructing the N400. *Nature Reviews Neuroscience*, *9*, 920–933.

Li, X., Hagoort, P., & Yang, Y. (2008). Event related potential evidence on the influence on the influence of accentuation in spoken discourse comprehension in Chinese. *Journal of Cognitive Neuroscience*, *20*, 906–915.

Luck, S. (2005). *An introduction to the event-related potential technique*. Cambridge, MA: MIT Press.

Makeig, S., Bell, A., Jung, T. P., & Sejnowski, T. (1996). Independent component analysis of electroencephalographic data. In D. Touretzky, M. Mozer, & M. Hasselmo (Eds.), *Advances in neural information processing systems* (pp. 145–151). Cambridge, MA: MIT Press.

Marinkovic, K., Dhond, R., Dale, A., Glessner, M., Carr, V., & Halgren, H. (2003). Spatiotemporal dynamics of modality-specific and supramodal word processing. *Neuron*, *38*, 487–497.

Maris, E., & Oostenveld, R. (2007). Nonparametric statistical testing of EEG and MEG data. *Journal of Neuroscience Methods*, *164*, 177–190.

Moreno, E., & Kutas, M. (2005). Processing semantic anomalies in two languages: An electrophysiological exploration in both languages of Spanish–English bilinguals. *Brain Research*, *22*, 205–220.

Oostenveld, R., Fries, P., Maris, E., & Schoffelen, J. M. (2011). FieldTrip: Open source software for advanced analysis of MEG, EEG, and invasive electrophysiological data. *Computational Intelligence and Neuroscience*, *2011*.

O'Rourke, T., & Holcomb, P. (2002). Electrophysiological evidence for the efficiency of spoken word processing. *Biological Psychology*, *60*, 121–150.

Pylkkänen, L., & Marantz, A. (2003). Tracking the time course of word recognition with MEG. *Trends in Cognitive Sciences*, *7*, 187–189.

Ruüsseler, J., Becker, P., Johannes, S., & Münte, T. (2007). Semantic, syntactic, and phonological processing of written words in adult developmental dyslexic readers: An event-related brain potential study. *BMC Neuroscience*, *8*, 1–10.

Simos, P., Basile, L., & Papanicolaou, A. (1997). Source localization of the N400 response in a sentence-reading paradigm using evoked magnetic fields and magnetic resonance imaging. *Brain Research*, *762*, 29–39.

Swaab, T., Brown, C., & Hagoort, P. (1997). Spoken sentence comprehension in aphasia: Event-related potential evidence for a lexical integration deficit. *Journal of Cognitive Neuroscience*, *9*, 39–66.

Tse, C., Lee, C., Sullivan, J., Garnsey, S., Dell, G., Fabiani, M., & Gratton, G. (2007). Imaging cortical dynamics of language processing with the event-related optical signal. *Proceedings of the National Academy of Sciences*, *104*, 17157–21716.

Vachon, F., & Jolicoeur, P. (2011). Impaired semantic processing during task-set switching: Evidence from the N400 in rapid serial visual presentation. *Psychophysiology*, *48*, 102–111.

van den Brink, D., Hagoort, P., & Brown, C. (2001). Electrophysiological evidence for early contextual influences during spoken-word recognition: N200 versus N400 effects. *Journal of Cognitive Neuroscience*, *13*, 967–985.

von der Malsburg, C. (1995). Binding in models of perception and brain function. *Current Opinion in Neurobiology*, *5*, 520–526.

Weber-Fox, C., & Neville, H. (1996). Maturational constraints on functional specializations for language processing: ERP and behavioral evidence in bilingual speakers. *Journal of Cognitive Neuroscience*, *8*, 231–256.